OPERATION OF SMALL RADIO TELESCOPE (SRT) RECORDED 21 CM SPECTRAL LINE OF HYDROGEN AT VATLY LABORATORY

Pham Ngoc Dong[a], Pham Tuan Anh[a], Pham Ngoc Diep[a], Pham Thi Tuyet Nhung[a] and Nguyen Van Hiep[b]

[a] *Institute for Nuclear Science and Technology, Vietnam Atomic Energy Institute*
[b] *Institute of Physics, VAST*

Project information:

- **Code: 24/CS/HĐ/NV**
- **Managerial Level: Institute**
- **Allocated Fund: 70,000,000 VND**
- **Implementation Time: 12 months (Jan 2012- Dec 2012)**
- **Contact Email: dongpn@mail.vinatom.gov.vn , ngocdong42@gmail.com**
- **Paper published in related to the project:**

1. Nguyen Van Hiep, *The VATLY radio telescope*, The Second Young Scientist's Conference on Nuclear Science and Technology, in Hanoi, October 2, 2012.
2. Nguyen Van Hiep *et al.*, *The VATLY radio telescope*, accepted for publication in Comm. Phys. Vietnam, (2012).

ABSTRACT: A small radio telescope (SRT) has been installed on the roof of the Hanoi astrophysics laboratory VATLY. It is equipped with a 2.6 m diameter mobile parabolic dish remotely controlled in elevation and azimuth and with super-heterodyne detection around the 21 cm hydrogen line. They demonstrate the high quality of the telescope performance and are used to evaluate lobe size, signal to noise ratios, anthropogenic interferences and measurement accuracies. Particular attention is given to the measurement of the pointing accuracy. First results of observations of the Sun and of the centre of the Milky Way are presented.

I. DESCRIPTION

In April 2012, a small radio telescope (SRT) has been installed on the roof of the VATLY astrophysics laboratory [1], commissioned and run-in. It is now routinely taking data. The present chapter presents its main features, illustrates its performance and provides evidence for excellent measuring conditions on both the continuum and the 21 cm hydrogen line.

Figure 1: Close-up views of the SRT antenna and of the motor system (gear box and telescopic arm, left panel) and of the feed horn and the calibration antenna (right panel).

The telescope is equipped with a mobile parabolic dish, 2.6 m in diameter, remotely adjustable in elevation and azimuth (Figure 1). The reflected power is collected at the focus, where

it is locally preamplified, shifted to lower frequency using standard superheterodyne, amplified and digitized. Standard data collection consists in a sequence of successive measurements of ~7.7 s duration each, digitized in the form of a frequency histogram covering ~1.2 MHz in 156 bins of ~7.8 kHz each. Such a typical distribution is shown in Figure 2 (left). The 21 cm hydrogen line is clearly seen above a slowly varying continuum. The hydrogen line signals the presence of hydrogen clouds in the field of view and is associated with electron spin flip in the hydrogen atom. Galaxies such as ours contain many such clouds and the signal from the Milky Way is particularly strong. On the contrary, the continuum signals the presence of ionized matter and is associated with thermal or "free-free" (bremsstrahlung) emission.

The following sections describe data collected on various targets including the Sun, with a strong continuum signal, and SgrA* at the centre of the Milky Way, with a strong 21 cm signal. They are used to illustrate and quantitatively evaluate the performance of the telescope and to sketch a programme of future observations. A preliminary account of this work was presented at recent conferences [2].

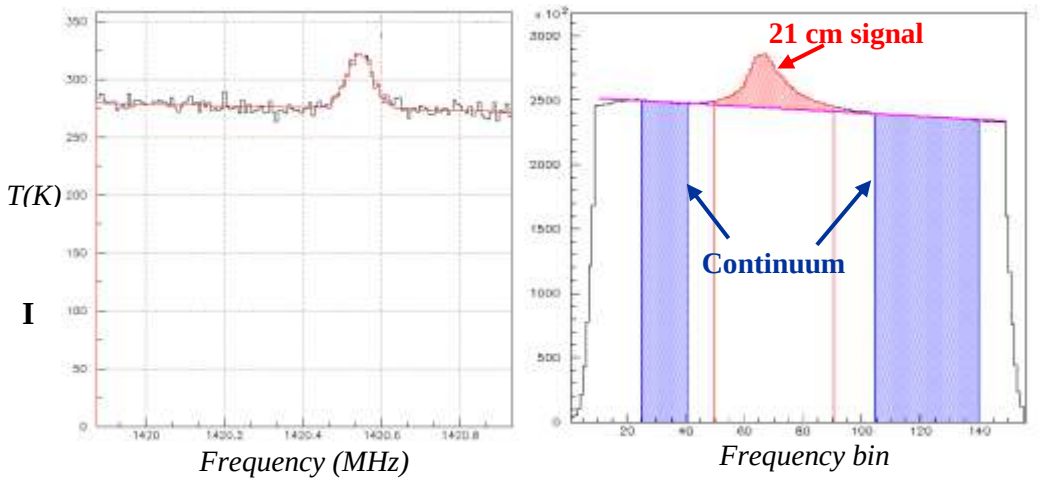

Figure 2: A typical frequency spectrum (left) and its decomposition in 21 cm and continuum signals (right).

II. GENERAL FEATURES

When pointing the telescope to a fixed direction in the sky, one records the sum of a general background and of signals associated with radio sources passing by as the Earth rotates (one speaks of drift scans). Examples of drift scans on the Sun and on Sgr A* respectively are illustrated in the next sections. In the present section, we are not interested in a particular radio source but rather in the contribution of the background.

However, while such pollution prevents reliable detection of the Sun in the 50 cm range [3], it can be easily handled in the present frequency band (which is officially protected). In the following, such spikes are removed from the data and the frequency distributions that are shown are free of parasite interferences. In order to illustrate the stability of the response, the distribution of the signal measured in a same frequency bin over a ~6.2 h period (after correction for slow drifts).

III. THE SUN: POINTING ACCURACY

The Sun gives a strong signal in the continuum while the 21 cm line is essentially unaffected. As its apparent diameter is much smaller than the antenna lobe (the Sun seen at 21 cm is dominated by solar spots above a disk having the same size as the photosphere) the Sun can be considered as being a point source. In the present section we use it to assess the SRT pointing accuracy.

3.1. Grid scans

In order to reveal possible pointing errors, 26 grid scans (Figure 3) have been made at different times of the day between April and June 2012. Each grid scan takes only 6 minutes and consists in 25 measurements pointing to the nodes of a 5×5 grid centred on the Sun and having a mesh size of ~2.6° (1/2 beam width) in elevation h and ~2.6°/cosh in azimuth a.

The scan of the grid is performed from east to west in lines of increasing elevation, with the SRT keeping pointing nominally to the node of the grid that is being measured. The nominal Sun is at the azimuth and elevation corresponding to the thirteenth grid node. The angular distance d_i between the true Sun and grid node i at the time when it is being measured is easily calculated by using the relation:

$$cosd=cos(h_1–h_2)–cosh_1cosh_2(1–cos(a_1–a_2) \quad (3.1)$$

which gives the angular separation between the directions (a_1,h_1) and (a_2,h_2).

Relation 3.1 reduces to:

$$d^2=(h_1–h_2)^2+ cosh_1cosh_2(a_1–a_2)^2 \quad (3.1')$$

in the limit of small angular separations: locally, one has a Euclidean metric in coordinates $(cosh\Delta a, \Delta h)$.

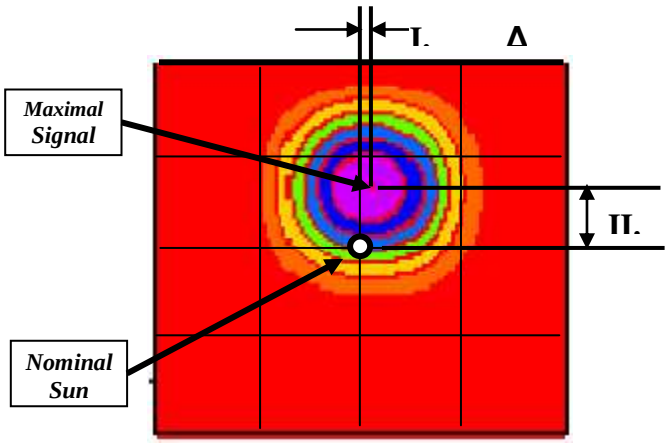

Figure 3: A typical grid scan: the 5×5 grid, centered on the nominal Sun, is shown together with the signal density in local coordinates $(dacosh,dh)$. The definition of the offsets is illustrated.

3.2. Parameterization

Two main causes come to mind to explain why δa and δh deviate significantly from zero: a possible tilt of the SRT rotation axis with respect to vertical and zero offsets of the azimuth and elevation scales. A tilt by an angle ε_0 in a plane of azimuth a_0 generates offsets

$$\delta a=–\varepsilon_0 sin(a–a_0)tanh \text{ and } \delta h=–\varepsilon_0 cos(a–a_0). \quad (3.2)$$

Defining $\varepsilon_1=\varepsilon_0 sina_0$ and $\varepsilon_2=\varepsilon_0 cosa_0$, one obtains $\delta a=\varepsilon_1 cosatanh–\varepsilon_2 sinatanh$ and $\delta h=–\varepsilon_1 sina–\varepsilon_2 cosa$ where both ε_1 and ε_2 are small angles.

We call ε_3 the zero offset of the azimuth scale. Rather than defining a zero offset of the elevation scale, it is better to define a zero offset ε_4 of the length of the telescopic arm that changes the elevation to which the SRT is pointing. This implies writing the zero offset of the elevation scale as $\varepsilon_4 \partial h/\partial l$ where the function $\partial h/\partial l$ has been calculated from the geometry of the movement:

$$\partial h/\partial l= –(7.9+0.666f)10^{–3}/g$$
$$\text{where } f=51.1–0.391h–0.00254h^2+0.77\ 10^{–5}h^3 \quad (3.3)$$
$$\text{and } g=\{1–(0.956–0.00792f–0.333\ 10^{–3}f^2)^2)^{½}$$

One can now express δa and δh in terms of four small parameters ε_i, which define the correction to apply to the nominal pointing direction of the SRT and are related to the azimuth and elevation offsets by the relations:

$$\delta a = \varepsilon_1 \cos a \tanh - \varepsilon_2 \sin a \tanh + \varepsilon_3$$
$$\delta h = -\varepsilon_1 \sin a - \varepsilon_2 \cos a + \varepsilon_4 \partial h / \partial l \qquad (3.4)$$

Here, the tilt angle is $\varepsilon_0 = (\varepsilon_1^2 + \varepsilon_2^2)^{1/2}$ and the azimuth of the tilt plane is $a_0 = \tan^{-1}(\varepsilon_1/\varepsilon_2)$.

The adequacy of the parameterization is illustrated where the measured offsets ($\cosh\delta a$, δh) are compared with those calculated by using the best fit values of the ε parameters:

$$\varepsilon_1 = 0.72 \pm 0.05, \quad \varepsilon_2 = 0.95 \pm 0.08, \quad \varepsilon_3 = -0.15 \pm 0.06, \quad \varepsilon_4 = -0.98 \pm 0.04 \qquad (3.5)$$

This corresponds to a tilt of $\varepsilon_0 = 1.2^o$ in the plane of azimuth 37.2^o. The rms values of the differences give a measure of the pointing error accuracy: $\cosh\Delta a = \Delta h = 0.15^o$.

The movement of the SRT dish is controlled by two motors to which one sends pulses, each pulse causing a step of 0.42^o in azimuth or 0.85 mm in the length of the telescopic arm, namely, at an elevation of 45^o, an angular step of $\sim 0.3^o$ (0.30^o in $\cosh\Delta a$ and 0.13^0 in elevation). The estimate of 0.15^o of the pointing accuracy obtained above corresponds therefore to half an average motor step, which is very reasonable.

3.3. Drift scans

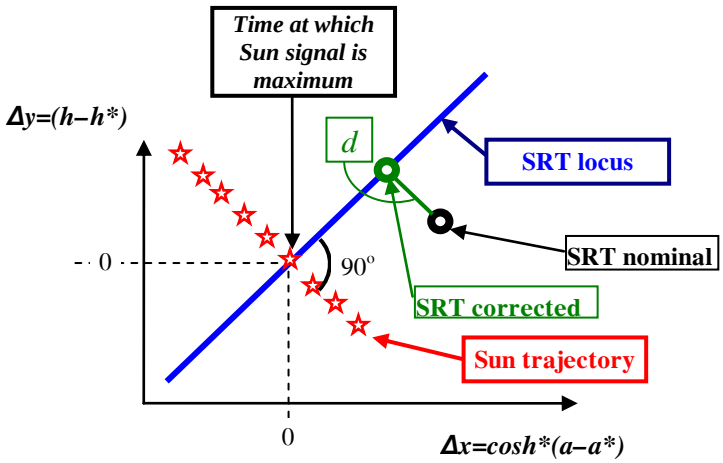

Figure 4: Schematic of a drift scan across the Sun. The quantity *d* measured by the scan is indicated.

For each of the 25 drift scans, the telescope was set to point to a given nominal Sun position during the whole duration of the scan, starting approximately half an hour before and ending approximately half an hour after the expected transit of the Sun at that point (Figure 4). This line is the locus of points for which the distance to the Sun trajectory is minimal at the point where the signal is maximal, namely the major circle normal to the Sun trajectory at the point where the signal is maximal.

Calling h^* and a^* the elevation and azimuth of this point and h and a the elevation and azimuth of the direction to which the SRT is pointing, the projection d on the Sun trajectory of the vector joining these two directions is a measure of the telescope offset. Precisely, calling $(\cos\theta, \sin\theta)$ the unit vector along the Sun trajectory in local coordinates $(da\cosh, dh)$,

$$d = (a - a^*)\cosh\cos\omega + (h - h^*)\sin\omega$$

The rms deviation of d around its mean is 1.2^o before and 0.3^o after applying the pointing corrections given by Relation 5. This illustrates the adequacy of the corrections and is consistent

with the rms values obtained from the grid scans. We retain an estimate of 0.3^o for the overall pointing accuracy.

IV. THE CENTRE OF THE GALAXY: A STRONG 21CM SIGNAL

Drift scans across the disk of the Milky Way give evidence for a strong 21 cm signal. The centre of the Galaxy contains a black hole, Sgr A*, having a mass of some 3 million solar masses; it is a strong radio source [4]. The disk of the Galaxy, and particularly its centre, contain a large number of hydrogen clouds that are the source of the observed 21 cm signal.

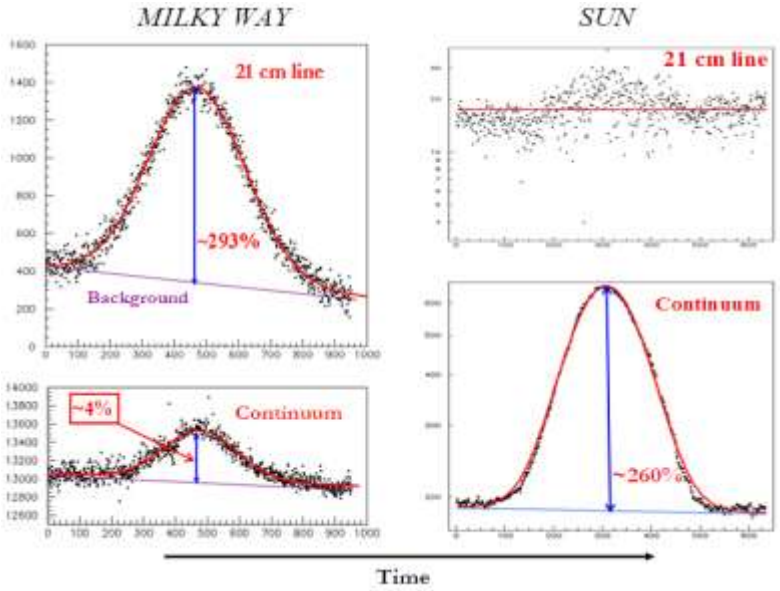

Figure 5: Drift scans across the centre of the Milky Way (left) and across the Sun (right). The 21 cm signal (upper panels) and the continuum signal (lower panels) are shown separately. The difference between the Milky Way, dominated by hydrogen clouds, and the Sun, dominated by hot plasma, is spectacular.

Figure 5 illustrates such a drift scan and compares it with a drift scan across the Sun. In the former case, there is only a small enhancement of the continuum, due to the much higher density of stars in the direction of Sgr A*, while the 21 cm signal is nearly tripled due to the presence of hydrogen clouds. In the Sun case, on the contrary, it is the continuum signal which is strongly enhanced, again by a factor of nearly 3, while the 21 cm signal is essentially unaffected (the small enhancement visible on Figure 5 is an artefact of our definition of the continuum signal, not going far enough on the tails of the Sun signal). Indeed, there is no enhancement of neutral hydrogen in the direction of the Sun.

The Sun has recently entered a new phase of activity after a long period of quietude [5]. Solar flares are associated with large radio bursts that tend to last longer than the visible flares [6]. Following the Sun radio emission over, say, two revolutions (namely ~2 months) will make it possible to detect such bursts and to compare them with their counterparts observed at other frequencies of the electromagnetic spectrum. The radio signals observed in both successive revolutions will be compared and correlated with existing solar spots in the field of view. Measurements across the disk of the Milky Way, repeated at different galactic longitudes, allow for a precise mapping of the hydrogen clouds in the SRT field of view and measurements of their radial velocities. Indeed, as illustrated in Figure 6, Doppler shifts of ~0.03 MHz can easily be measured, corresponding to radial velocities of ~7 km/s, much smaller than typical relative radial velocities in the Galaxy.

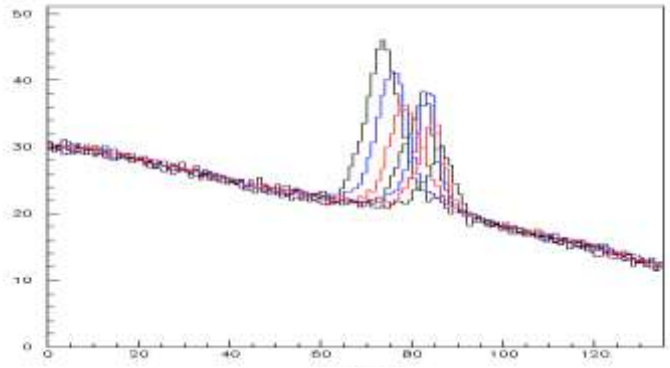

Figure 6: Frequency spectra showing the sensitivity to different Doppler shifts of the 21 cm line.

Moreover, other radio sources can be observed [7] and their 21 cm and continuum signals can be measured. These include in particular nearby galaxies such as Andromeda, nearby Active Galactic Nuclei such as Cen A [8] and young Super Nova remnants such as Cassiopeia and the Crab.

REFERENCES

[1] Produced by Custom Astronomical Support Services, Inc.

[2] N.V.Hiep (on behalf of VATLY) presented at the 1st Southeast Asian Young Astronomers Collaboration (SEAYAC) Meeting, Puerto Princesa City, Palawan, Philippines, November 5-9, 2012.

N.V. Hiep et al., *The VATLY radio telescope*, (2012) to appear in Comm. Phys. Vietnam.

[3] P.T. Anh, Radio Detection of the Sun, Master thesis presented at the Institute of Physics, Hanoi, September 2010.

[4] K. T. Phuong, *The Black Hole in the Centre of the Milky Way*, Diploma 2006.

[5] http://www.n3kl.org/sun/noaa.html; http://www.n3kl.org/sun/status.html;

http://www.universetoday.com/10846/predicting-times-for-clear-space-weather.

[6] R.E. Loughhead, J.A. Roberts and M.K. McCabe, *The Association of Solar Radio Bursts of Spectral Type III with Chromospheric Flares*, Aus. J. Phys. 483, 10, 1957.

R. Hill, *Observing Solar White Light Flares*, http://www.alpo-astronomy.org/ solarblog/?page_id=200.

[7] R.X. McGee, J.D. Murray and J.A. Milton, *A Sky Survey of Neutral Hydrogen at 21 cm*, Aust. J. Phys. 16, 136, 1963.

[8] L. T. Huong, *Galaxy Collisions as Possible Sources of Ultra High Energy Cosmic Rays*, Dissertation presented at the Hanoi National University of Education, 2008.